Occurrence of Hyperon Superfluidity in Neutron Star Cores *

Tatsuyuki TAKATSUKA[1], Shigeru NISHIZAKI[1],
Yasuo YAMAMOTO[2] and Ryozo TAMAGAKI[3]

[1]*Faculty of Humanities and Social Sciences, Iwate University, Morioka 020-8550, Japan*
[2]*Physics Section, Tsuru University, Tsuru 402-8555, Japan*
[3]*Kamitakano Maeda-Cho 26-5, Kyoto 606-0097, Japan*

(Received)

Superfluidity of Λ and Σ^- admixed in neutron star (NS) cores is investigated realistically for hyperon (Y)-mixed NS models obtained by a G-matrix-based effective interaction approach. The equation of state (EOS) with the mixing ratios of respective components and also hyperon energy gaps including the temperature dependence are numerically presented in order to serve as physical inputs for Y-cooling calculations of NSs. By covering the uncertainties of the EOS and the YY interactions, it is shown that both of Λ and Σ^- are superfluid as soon as they appear although the magnitude of critical temperature and the existent density region considerably depend on the YY pairing potential. From the viewpoints of momenturm triangle condition and the occurrence of superfluidity, a so-called "hyperon cooling" (neutrino-emission from direct Urca process including Y) combined with Y-superfluidity is found to be a promising candidate to explain observations of colder class NSs, together with a remark that Λ-hyperons play a decisive role in the hyperon cooling scenario. Some comments are given as to the consequence of less attractive $\Lambda\Lambda$ interaction recently suggested by the "NAGARA event" ${}^{6}_{\Lambda\Lambda}$He.

§1. Introduction

Neutron stars (NSs) are primarily composed of predominant neutrons and small amount of protons, coexisting with electrons and muons to assure the charge neturality of the system. With the increase of total baryon density ρ toward the central region, however, hyperons (Y) such as Λ, Σ^- and Ξ^- begin to appear as new components. This is because the chemical potential of the predominating neutron component gets higher with ρ and eventually it becomes energetically economical for the system to replace neutrons at the Fermi surface by Y through a strangeness non-conserving weak interaction, in spite of the cost of higher rest-mass energy. The population of Y increases with increasing ρ and hyperons become important constituents of NS cores, as well as nucleons.

Internal composition and structure strongly affect the thermal evolution of NSs, and much attention has continuously been paid to this problem from various viewpoints.[4)-18)] The participation of Y is to provide much faster cooling mechanism due to the very efficient neutrino-emission processes,[19)] the so-called "hyperon direct Urca" (abbreviated to as Y-DUrca; e.g., $\Lambda \to p + l + \bar{\nu}_l$, $\Sigma^- \to \Lambda + l + \bar{\nu}_l$ and their inverse processes; $l \equiv e^-$ or μ^-), compared to the standard cooling mechanism,

* A part of this work has been reported in Refs. 1)- 3).

called the "modified Urca" (MUrca; e.g., $n+n \to n+p+l+\bar{\nu}_l$, $n+p \to p+p+l+\bar{\nu}_l$ and their inverse processes). The ν-emission rate for the hyperon cooling (Y-DUrca) is larger by 5-6 orders of magnitude than that for the standard cooling (MUrca), because in the latter an additional nucleon has to join in the β-decay process in order to satisfy the momentum conservation for the reactions. This rapid hyperon cooling is of particular interest in relation to the surface temperature observations of NSs. That is, recent observations suggest that there are at least two classes of NSs, hotter ones and colder ones and are stimulationg studies on cooling scenarios to explain two classes consistently. The standard cooling, together with some frictional heating mechanism, can explain the hotter ones, but cannot the colder ones. [10] Then the fast non-standard hyperon cooling shows up as a candidate to explain the colder ones. A direct action of the hyperon cooling, however, leads to a serious problem of "too rapid cooling" incompatible with observations and therefore some suppression mechanism for an enhanced ν-emission rate is vital. A most natural candidate to play this supprression role is the hyperon superfluidity.

In this paper, we study whether hyperons admixed can be superfluids or not and show that this is the case. [1) - 3)] This means that the hyperon cooling scenario, combined with the Y-superfluidity, is a promising candidate for the fast non-standard cooling compatible with the data of the colder class NSs. In our preceding works, [20) - 22)] we discussed the hyperon energy gap Δ_Y responsible for Y-superfluids by a simplied treatment where the ρ-dependent Y-mixing ratios $y_Y (\equiv \rho_Y/\rho)$ relevant to the Fermi momontum k_{FY} and ρ-dependent effective-mass parameter m_Y^* are taken as parameters. In the present work, we use the ρ-dependent $y_Y(\rho)$ and $m_Y^*(\rho)$ based on the Y-mixed NS models in order to get the realistic Δ_Y in a ρ-dependent way. Also, we present the profile functions representing the temperature-dependence of Δ_Y, which is necessary for treating the thermal evolution of NSs, and intend to provide the basic physical quantities for cooling calculations in a realistic level.

This paper is organized as follows. In §2, our NS models with Y-mixing, calculated by a G-matrix effective interaction approach, are presented, together with the composition, the equation of state (EOS) and the physical quantities necessary for the energy gap calculations. The energy gap equation including a finite-temperature ($T > 0$) case is treated in §3, where some comments are given on the impotant ingredients in the gap equation, i.e., $m_Y^*(\rho)$ and the YY pairing interactions in comparison with the case of nucleons. Results of Δ_Y and the profile functions are given in §4, together with discussions as to the momentum triangle condition for Y-DUrca processes and the superfluid suppression on ν-emissivities. In addition, in §5, we discuss how a less attractive $\Lambda\Lambda$ interaction inferred from ${}^{6}_{\Lambda\Lambda}$He observed recently affects the realization of Y superfluidities. The last section, §6, is for summary and remarks.

§2. Neutron Star Models with Hyperons

We calculate the EOS of Y-mixed NS matter responsible for Y-mixed NS models and also obtain the ρ-dependent y_Y and m_Y^* of hyperons necessary for the energy gap calculations. For simplicty, we neglect the mixing of Ξ^- component and restrict

ourselves to $Y \equiv \{\Lambda,\ \Sigma^-\}$ as the hyperon components, since it would be less likely for Ξ^- to appear due to the higher mass ($m_{\Xi^-} = 1321$ MeV compared to $m_\Lambda = 1116$ MeV and $m_{\Sigma^-} = 1192$ MeV). We treat the Y-mixed NS matter composed of n, p, Λ, Σ^-, e^- and μ^- by a G-matrix based effective interaction approach, with attention to the use of YN and YY interactions compatible with hypernuclear data: [23) - 25)]

1. We construct the effective YN and YY local potentials, $\tilde{V}_{YN}$ and $\tilde{V}_{YY}$, in a ρ- and y_Y-dependent way, from the G- matrix calculations performed for $\{n+Y\}$ matter with a given ρ and y_Y. In these calculations, we use the YN and YY interactions from the Nijmegen model D hard core potential [26)] (NHC-D) with a slight modification in the S-state ΛN part (NHC-Dm) as a reasonable choice (details are refered to Ref. 23)). From a view of Λ effective-mass parameter (m^*_Λ) controlling the realization of Λ-superfluidity which will be discussed in the next section, the choice of this NHC-Dm is adequate since it reproduces $m^*_\Lambda \sim 0.8$ infered from hypernuclear data. [27)]
2. For the effective NN local potential $\tilde{V}_{NN}$, we use $\tilde{V}_{\rm RSC}$ supplemented by $\tilde{V}_{\rm TNI}$, i.e., $\tilde{V}_{NN} = \tilde{V}_{\rm RSC} + \tilde{V}_{\rm TNI}$ where $\tilde{V}_{\rm RSC}$ [28)] is the effective two- nucleon potential constructed from the G-matrix calculations in asymmetric nuclear matter with the Reid-soft-core potential and $\tilde{V}_{\rm TNI}$ [29)] is a phenomenological three-nucleon interaction (TNI) of Lagaris-Pandharipande type. [30), 31)] The $\tilde{V}_{\rm TNI}(= \tilde{V}_{\rm TNA} + \tilde{V}_{\rm TNR})$ consists of two parts, the attractive $\tilde{V}_{\rm TNA}$ and the repulsive $\tilde{V}_{\rm TNR}$ and expressed in a form of two-body potential with ρ-dependence. At high densities the contribution from $\tilde{V}_{\rm TNA}$ is minor and that from $\tilde{V}_{\rm TNR}$ dominates and TNI brings a strong repulsion with increasing ρ. The parameters inherent in $\tilde{V}_{\rm TNI}$ are determined so that $\tilde{V}_{\rm TNI}$ can reproduce the empirical saturation properties of symmetric nuclear matter (binding energy $E_{\rm B} = -16$ MeV and saturation density $\rho_0 \equiv 0.17$ nucleons/fm^3) and the nuclear incompressibility κ.
3. On the basis of $\tilde{V}_{NN}$, $\tilde{V}_{YN}$ and $\tilde{V}_{YY}$, we calculate the fractions y_i for respective components ($i = n$, p, Λ, Σ^-, e^- and μ^-) in β-equilibrium, under the conditions of charge neutrality, chemical equilibrium and baryon number conservation, and derive the EOS and $m^*_Y(\rho)$ of Y-mixed NS matter.

By using the EOS thus obtained, we solve the so-called TOV equation and obtain NS models with a Y-mixed core. Our NS models are specified by the parameter κ relevant to $\tilde{V}_{NN}$, which is a measure for the stiffness of a nuclear-part EOS (N-part EOS). We consider three cases; $\kappa = 250$ MeV (hereafter, denoted by TNI2), 300 MeV (TNI3) and 280 MeV (TNI6). TNI2 is a soft EOS case, TNI3 is a stiffer EOS case and TNI6 is between the two, giving respectively the maximum mass $M_{\rm max}$ of NSs sustained by the EOS as $M_{\rm max} \simeq 1.62 M_\odot$, $1.88 M_\odot$ and $1.78 M_\odot$ for normal NSs without Y-mixing. In Fig.1, we compare our EOSs for neutron matter with those by Illinoi group currently taken as most realistic. We stress that our EOSs almost cover the range from soft to stiff cases allowed by realistic EOSs from more sophisticated many-body approach. [32), 33)]

As a peculiar property for the Y-mixed NS models, we wish to remark that the Y-mixing casuses a dramatic softening effect on the EOS and thereby $M_{\rm max}$ for Y-mixed NSs is greatly reduced. [23) - 25)] For example, $M_{\rm max} \simeq 1.62 M_\odot$ for the case without Y is reduced to $M \simeq 1.08 M_\odot$ for the case with Y, contradicting the condition that

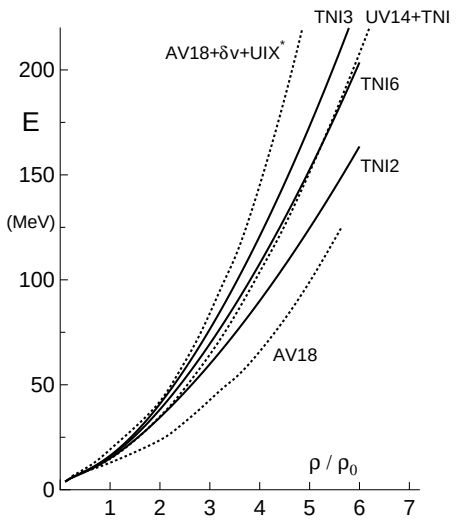

Fig. 1. Energy per particle E versus density ρ, corresponding to the EOS of neutron matter ($\rho_0 = 0.17$ nucleons/fm^3 being the nuclear density). Solid lines with TNI2, TNI6 and TNI3 are respectively soft, intermediate and stiff EOSs considered here. EOSs from Illinois group, i.e., AV18 [33] (softest), UV14+TNI [32] (intermediate) and AV18+δv+UIX [33] (stiffest), are also displayed by dotted lines showing that our EOSs are well in the range from softest to stiffest EOS currently taken as realistic.

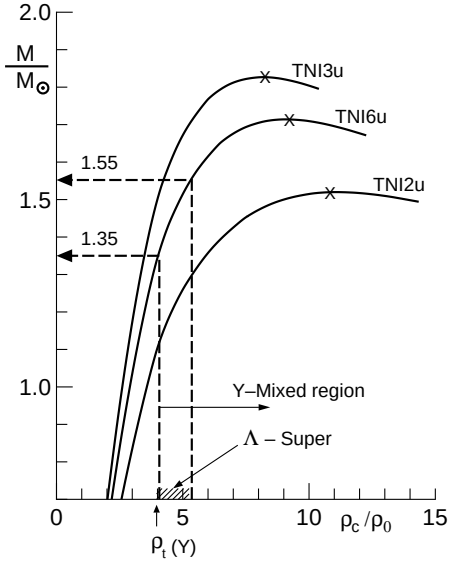

Fig. 2. Mass M versus central density ρ_c for neutron stars (NSs) corresponding to the EOS of hyperon (Y)-mixed neutron star matter (TNI2u, TNI6u and TNI3u) where repulsion from three-nucleon interaction (TNI) are introduced universaly (details are in text). Crosses denote the maximum mass point. The threshold density $\rho_t(Y)$ of Y-mixing and existence density region of Λ-superfluid for ND-Soft pairing interaction are also shown to indicate the M- and EOS- dependence of Λ-superfluid phase.

at least $M_{\rm max}$ should be larger than $M_{\rm obs}$(PSR1913+16)=$1.44M_\odot$, the observed NS mass for PSR1913+16. This inconsistency between theory and observation cannot be resolved by using a stronger NN repulsion as seen from $M_{\rm max} \simeq 1.08M_\odot \to 1.09M_\odot \to 1.10M_\odot$ for TNI2$\to$TNI6 $\to$TNI3 with increasing κ. This is because the stiffer the N-part EOS, the Y-mixed phase developes from lower densities and thereby the softening effect becomes all the stronger, making the enhanced NN repulsion ineffective. The problem of $M_{\rm max} < M_{\rm obs}$ for Y-mixed NSs is also seen in other approaches [34),35)] and is encountered almost in a model-independent way, which interestingly suggests that some "extra repulsion" has to work for hypernuclear systems, namely, YN and YY interaction parts. As one of the candidates, we try to introduce a repulsion from the three-body force $\tilde{V}_{\rm TNR}$ in TNI also into the YN and YY parts, as well as NN part (hereafter called "universal inclusion of TNI" and denoted simply by TNIu), [23)-25)] since the importance of three-body interaction is well recognized for nuclear systems and should not be restricted to nuclear systems (NN part). Then, we have a moderate softening, not a dramatic one as before, and a larger $M_{\rm max}$ nicely satisfying the condition $M_{\rm max} > 1.44M_\odot$; $M_{\rm max} \simeq 1.52M_\odot$,

$1.71M_\odot$ and $1.83M_\odot$ for TNI2u, TNI6u and TNI3u, respectively. We also note that the realization of a Y-mixed phase is pushed to higher density side; the threshold density $\rho_t(Y) \simeq (2.5-3)\rho_0$ for no extra repulsion whereas $\rho_t(Y) \simeq 4\rho_0$ for the universal inclusion of three-body repulsion. These aspects suggest that $\rho_t(Y)$ is not so low as currently taken ($\rho_t(Y) \sim 2\rho_0$) but is rather high ($\sim 4\rho_0$) as far as the consistency with the NS mass observation is taken into account.[25] In Table I, we summarize the parameters profiling the Y-mixed NSs having the maximum mass $M_{\rm max}$ and illustrate in Fig.2 the M-ρ_c relationships indicating how the Y-mixed core region depends on M and EOS. We give in Table II the numerical values of composition and EOS for Y-mixed NSs.

Table I. Profile (mass $M_{\rm max}$, radius R and central density ρ_c) of maximum-mass NSs in Fig.2 for EOSs from soft (TNI2u) to stiff (TNI3u). The thresold density $\rho_t(Y)$ indicating the portion of Y-mixed core is also shown for Λ and Σ^- cases.

EOS	$\rho_{\rm t}(\Lambda)/\rho_0$	$\rho_{\rm t}(\Sigma^-)/\rho_0$	$M_{\rm max}/M_\odot$	R/km	$\rho_{\rm c}/\rho_0$
TNI2u	4.01	4.06	1.52	8.43	11.08
TNI6u	4.02	4.06	1.71	9.16	9.07
TNI3u	4.01	4.01	1.83	9.55	8.26

Table II. (a) EOS of Y-mixed NS matter with the mixing ratio y_i of the constituents ($i = n$, p, Λ, Σ^-, e^-, μ^-). The energy density e is in MeV/fm^3 and the pressure P is in dyn/cm^2, for the case of TNI2u.

ρ/ρ_0	$y_{\rm n}$	$y_{\rm p}$	y_Λ	$y_{\Sigma-}$	$y_{\rm e-}$	$y_{\mu-}$	e	P
0.5	0.9684	0.0316	0.	0.	0.0316	0.	80.5	5.51E+32
1.0	0.9499	0.0501	0.	0.	0.0451	0.0050	161.9	3.67E+33
1.5	0.9409	0.0591	0.	0.	0.0464	0.0128	244.9	1.13E+34
2.0	0.9380	0.0620	0.	0.	0.0453	0.0168	330.1	2.40E+34
2.5	0.9371	0.0629	0.	0.	0.0439	0.0191	417.6	4.23E+34
3.0	0.9368	0.0632	0.	0.	0.0426	0.0206	507.7	6.70E+34
3.5	0.9368	0.0632	0.	0.	0.0415	0.0216	600.9	9.92E+34
4.0	0.9371	0.0629	0.	0.	0.0406	0.0224	697.2	1.40E+35
4.5	0.8561	0.0862	0.0262	0.0315	0.0354	0.0193	796.8	1.80E+35
5.0	0.7633	0.1127	0.0574	0.0667	0.0301	0.0159	899.2	2.25E+35
5.5	0.6824	0.1354	0.0859	0.0963	0.0258	0.0133	1004.8	2.78E+35
6.0	0.6135	0.1545	0.1109	0.1211	0.0223	0.0111	1113.5	3.38E+35
6.5	0.5556	0.1701	0.1327	0.1416	0.0193	0.0092	1225.6	4.08E+35
7.0	0.5071	0.1827	0.1518	0.1584	0.0167	0.0076	1341.3	4.87E+35
7.5	0.4660	0.1929	0.1687	0.1723	0.0144	0.0062	1460.7	5.77E+35
8.0	0.4308	0.2013	0.1838	0.1840	0.0123	0.0049	1584.1	6.77E+35
9.0	0.3734	0.2143	0.2096	0.2027	0.0088	0.0028	1843.3	9.10E+35
10.0	0.3277	0.2243	0.2309	0.2170	0.0060	0.0013	2120.3	1.19E+36
11.0	0.2898	0.2329	0.2485	0.2288	0.0038	0.0003	2416.3	1.52E+36
12.0	0.2570	0.2410	0.2631	0.2388	0.0022	0.0000	2732.5	1.90E+36
13.0	0.2272	0.2492	0.2754	0.2481	0.0011	0.0000	3069.9	2.34E+36
14.0	0.1983	0.2581	0.2859	0.2577	0.0004	0.0000	3429.3	2.82E+36
15.0	0.1675	0.2689	0.2948	0.2688	0.0001	0.0000	3811.6	3.36E+36

Table II. (b) Same as in (a) but for TNI6u case.

ρ/ρ_0	$y_{\rm n}$	$y_{\rm p}$	y_Λ	y_{Σ^-}	$y_{\rm e^-}$	y_{μ^-}	e	P
0.5	0.9682	0.0318	0.	0.	0.0318	0.	80.5	5.87E+32
1.0	0.9473	0.0527	0.	0.	0.0468	0.0058	162.0	4.00E+33
1.5	0.9369	0.0631	0.	0.	0.0488	0.0143	245.4	1.31E+34
2.0	0.9341	0.0659	0.	0.	0.0475	0.0184	331.2	2.91E+34
2.5	0.9341	0.0659	0.	0.	0.0455	0.0203	420.2	5.26E+34
3.0	0.9349	0.0651	0.	0.	0.0437	0.0214	512.6	8.47E+34
3.5	0.9358	0.0643	0.	0.	0.0421	0.0221	608.8	1.27E+35
4.0	0.9366	0.0634	0.	0.	0.0408	0.0226	709.2	1.80E+35
4.5	0.8550	0.0869	0.0261	0.0321	0.0354	0.0193	814.0	2.37E+35
5.0	0.7609	0.1136	0.0578	0.0677	0.0300	0.0159	923.0	3.02E+35
5.5	0.6797	0.1363	0.0865	0.0975	0.0257	0.0132	1036.4	3.79E+35
6.0	0.6110	0.1553	0.1116	0.1222	0.0221	0.0109	1154.5	4.68E+35
6.5	0.5534	0.1707	0.1334	0.1425	0.0191	0.0091	1277.6	5.71E+35
7.0	0.5052	0.1831	0.1525	0.1591	0.0165	0.0075	1406.1	6.89E+35
7.5	0.4645	0.1932	0.1694	0.1729	0.0142	0.0061	1540.1	8.23E+35
8.0	0.4296	0.2015	0.1845	0.1845	0.0122	0.0048	1680.0	9.73E+35
9.0	0.3725	0.2144	0.2102	0.2029	0.0087	0.0028	1978.6	1.32E+36
10.0	0.3271	0.2244	0.2313	0.2172	0.0059	0.0013	2304.1	1.75E+36
11.0	0.2893	0.2330	0.2489	0.2289	0.0038	0.0003	2658.3	2.25E+36
12.0	0.2566	0.2411	0.2635	0.2389	0.0022	0.0000	3043.3	2.83E+36

Table II. (c) Same as in (a) but for TNI3u case.

ρ/ρ_0	$y_{\rm n}$	$y_{\rm p}$	y_Λ	y_{Σ^-}	$y_{\rm e^-}$	y_{μ^-}	e	P
0.5	0.9681	0.0319	0.	0.	0.0319	0.	80.5	6.17E+32
1.0	0.9454	0.0546	0.	0.	0.0481	0.0065	162.1	4.21E+33
1.5	0.9334	0.0666	0.	0.	0.0509	0.0158	245.6	1.42E+34
2.0	0.9302	0.0698	0.	0.	0.0498	0.0201	332.0	3.26E+34
2.5	0.9306	0.0694	0.	0.	0.0475	0.0219	422.0	6.01E+34
3.0	0.9321	0.0679	0.	0.	0.0452	0.0226	516.0	9.80E+34
3.5	0.9339	0.0661	0.	0.	0.0432	0.0230	614.5	1.48E+35
4.0	0.9354	0.0646	0.	0.	0.0415	0.0231	718.1	2.11E+35
4.5	0.8457	0.0907	0.0274	0.0362	0.0353	0.0192	826.8	2.79E+35
5.0	0.7516	0.1172	0.0594	0.0718	0.0297	0.0157	940.6	3.59E+35
5.5	0.6712	0.1395	0.0881	0.1012	0.0254	0.0129	1059.8	4.54E+35
6.0	0.6038	0.1578	0.1132	0.1253	0.0218	0.0107	1184.9	5.65E+35
6.5	0.5475	0.1726	0.1349	0.1449	0.0189	0.0089	1316.2	6.94E+35
7.0	0.5004	0.1846	0.1539	0.1611	0.0163	0.0073	1454.2	8.41E+35
7.5	0.4605	0.1943	0.1707	0.1744	0.0140	0.0059	1599.1	1.01E+36
8.0	0.4263	0.2023	0.1857	0.1857	0.0120	0.0047	1751.3	1.19E+36
9.0	0.3702	0.2148	0.2113	0.2037	0.0085	0.0027	2079.3	1.63E+36
10.0	0.3255	0.2246	0.2322	0.2177	0.0058	0.0012	2440.9	2.17E+36

§3. Energy gap equation for hyperon pairing

As shown in the preceding section, hyperons participate at high densities ($\rho \gtrsim \rho_t(Y) \sim 4\rho_0$) but the fractional density $\rho_Y (= y_Y \rho)$ is relatively low due to small

contamination, e.g., $y_Y \lesssim 0.1$ for the density region $\rho \simeq (\rho_t(Y) \sim 6\rho_0)$ of interest. Then the scattering energy $E_{YY}^{\rm lab}$ in laboratory frame for a ($\vec{q}$, -$\vec{q}$)- Cooper pair near the Fermi surface ($q \simeq q_{FY} = (3\pi^2\rho_Y)^{1/3}$ with q_{FY} being the Fermi momentum of Y) is at most 110 MeV, estimated by $E_{YY}^{\rm lab} = 4E_{FY} = 4\hbar^2 q_{FY}^2/2M_Y$ with E_{FY} and M_Y being the Fermi kinetic energy and the mass of hyperons, respectively. This means that the pairing interaction V_{YY} responsible for Y-superfluidity should be that in the $^1S_0$ pair state ($V_{YY}(^1S_0)$) which is most attractive at low scattering energies. Thus the gap equation to be treated here is the well-known $^1S_0$-type:

$$\Delta_Y(q) = -\frac{1}{\pi}\int_0^\infty q'^2 dq' < q' \mid V_{YY}(^1S_0) \mid q > \frac{\Delta_Y(q')}{E_Y(q')} \tanh\left(\frac{E_Y(q)}{2\kappa_{\rm B}T}\right), \quad (3\cdot1)$$

$$E_Y(q') \equiv \sqrt{\tilde{\epsilon}_Y^2(q') + \Delta_Y^2(q')}, \quad (3\cdot2)$$

$$\tilde{\epsilon}_Y(q') \equiv \epsilon_Y(q') - \epsilon_Y(q_{FY}) \simeq \frac{\hbar^2}{2M_Y^*}(q'^2 - q_{FY}^2), \quad (3\cdot3)$$

$$< q' \mid V_{YY}(^1S_0) \mid q > \equiv \int_0^\infty r^2 dr j_0(q'r) V_{YY}(r;^1S_0) j_0(qr), \quad (3\cdot4)$$

including the case of finite temperature with $\kappa_{\rm B}$ being the Boltzman constant. In the above expressions, $\Delta_Y(q)$ is the energy gap function, $\epsilon_Y(q)$ the single-particle energy and M_Y^* the effective mass of Y. For simplicity, the effective mass approximation for $\epsilon_Y(q)$ is adopted in Eq.(3·3). We use a bare $V_{YY}(^1S_0)$ for pairing interaction and do not introduce the G-matrix based effective interaction $\tilde{V}_{YY}(^1S_0)$ in place of $V_{YY}(^1S_0)$ as adopted by Balberg-Barnea,[36] because the gap equation plays dual roles to take account of the pairing correlation and the short-range correlation (s.r.c.) at the same time and so the use of $\tilde{V}_{YY}(^1S_0)$ leads to incorrect results with larger energy gaps due to the double counting of s.r.c..

The gap equation (Eq.(3·1)) is solved numerically when q_{FY}, M_Y^* and $V_{YY}(^1S_0)$ are given. We solve it exactly without any approximation by an iterative technique. The q_{FY} (equivalently y_Y) and M_Y^* (equivalently the effective mass parameter $m_Y^* \equiv M_Y^*/M_Y$) are derived in §2. In the following, we give some notices to the important ingredient in Eq.(3·1), m_Y^* and $V_{YY}(^1S_0)$, controlling the resulting energy gap $\Delta_Y \equiv \Delta_Y(q_{FY})$.

i) effective mass parameter m_Y^*

Generally, energy gap is very sensitive to m_Y^* and results in a larger value for larger m_Y^*. This is due to that the energy cost for the excitation of YY-pair($\tilde{\epsilon}_Y(q)$ in Eq.(3·3)) is smaller for larger $M_Y^*(\equiv m_Y^* M_Y)$. In this sense, the Y-superfluidity is more likely to occur, compared to that of nucleons, since $m_Y^* \simeq (0.8 \sim 1.2)$ is remarkably larger than $m_N^* \simeq (0.5 \sim 0.7)$ at $\rho \gtrsim 4\rho_0$ as shown in Fig.3. Moreover the fact that $M_Y \simeq$ (1116 MeV or 1192 MeV)$> M_N \simeq 940$ MeV enforces this advantage. It is of interest to note that $m_Y^* = 0.8$ corresponds to $m_N^* = (M_Y/M_N)m_Y^* \simeq 1.0$ for

$Y \equiv \Sigma^-$ case. Comparison between the Λ and Σ^- cases tells us that Σ^--superfluidity is more favourable than Λ-superfluidity since $m^*_{\Sigma^-} > m^*_\Lambda$ and in addition $M_{\Sigma^-} > M_\Lambda$. That is, the resulting energy gaps for baryon superfluids are as $\Delta_{\Sigma^-} > \Delta_\Lambda > \Delta_N$, as far as the role of effective mass is concerned.

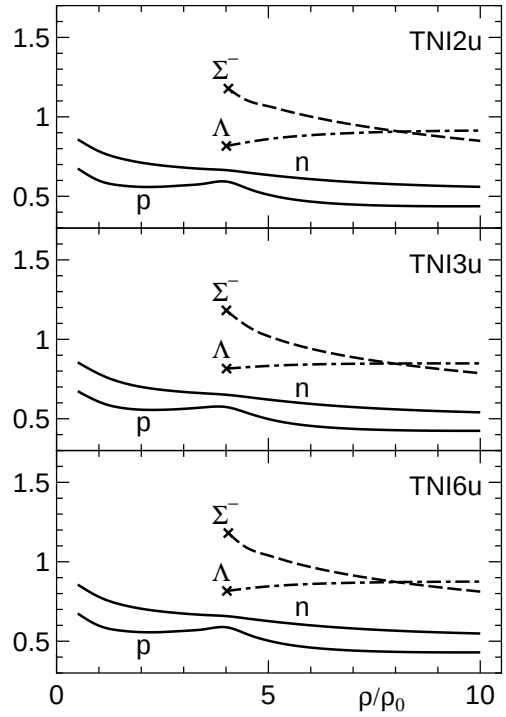

Fig. 3. Effective mass parameter m^*_i for baryon components ($i = n$, p, Λ, Σ^-) as a function of ρ for three cases (TNI2u, TNI6u, TNI3u) of Y-mixed NS matter with different stiffness. Crosses denote the threshold points for the Y-mixing.

(ii) Pairing potential

The attractive effect of the YY pairing potential $V_{YY}(^1S_0)$ is a main agency for the occurrence of Y-superfluidity. Our present knowledge of $V_{YY}(^1S_0)$, however, is very limited. As in previous works, we adopt three potentials called ND-Soft [37),21),2)] ** , Ehime [38)] and FG-A, [39)] expecting to cover the present uncertainties of YY potentials. They are commonly based on the one-boson-exchange (OBE) hypothesis with SU(3) symmetry in the framework of nonet mesons and octet baryons (B). Main differences among them are in the treatments of short-range interactions and the kinds of mesons introduced. The ND-Soft potential is a soft-core version of the original Nijmegen hard-core model D (NHC-D) [26)] by a superposition of three-range Gaussian functions and is constructed so as to fit the t-matrix from NHC-D with thw hard-core radii being taken as 0.5fm. The use of soft-core version is for the sake of convenience in the treatment of the gap equation. The Ehime potential is

** In the Table I of Ref. 2), $V^c_{i\Sigma^-}$ with $i = 2$ should be corrected as $-2.9232 \to -29.232$.

characterized by an application of the OBE scheme throughout all the interaction ranges and by an addition of a phenomenological neutral scalar meson to take the 2π-correlation effects of this sort into account. It is given by a superposition of the Yukawa-type functions in r-space regularized by the form factors in momentum space and has velocity-dependent terms. The FG-A potential is based on the OBE-scheme where the σ-meson is treated in the nonet scheme, by taking account of the broad width of σ- and ρ-mesons, and has a Gausian soft-core repulsion with strengths constrained by the SU(3) representation of two-baryons. This potential includes the velocity-dependence and the retardation effects.

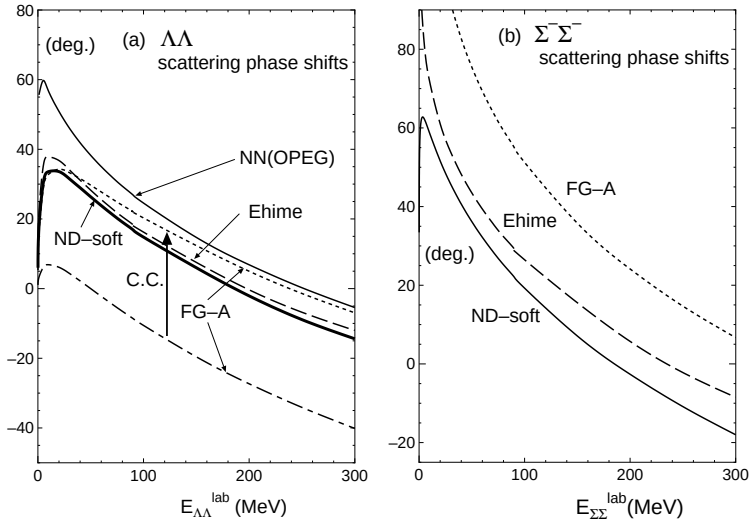

Fig. 4. (a) $\Lambda\Lambda$ scattering phase shifts in degrees as a function of laboratory frame energy $E^{\rm lab}_{\Lambda\Lambda}$ in MeV for three $\Lambda\Lambda$ $^1S_0$ potentials (ND-Soft, Ehime and FG-A) explained in the text. NN scattering phase shifts from OPEG-^{1}E potential are also shown for comparison. The $\Lambda\Lambda$-$\Sigma^-\Sigma^-$-$\Xi^-\Xi^-$ channel coupling (CC) effects are shown by the arrow for the FG-A case (The long dash-dotted lline is for no CC.). (b) Same as in (a) but for $\Sigma^-\Sigma^-$ scattering.

Here we add a comment on the treatment of the channel coupling effect (CCE) of $\Lambda\Lambda$-$\Sigma\Sigma$-ΞN type in these potentials. The ND-Soft is constructed so as to simulate the t-matrices calculated with the NHC-D in $\Lambda\Lambda$ and ΞN channels. For simplicity, here, we use only the $\Lambda\Lambda$-$\Lambda\Lambda$ diagonal part of ND-Soft, because the $\Lambda\Lambda$-ΞN coupling effect was found to be small for the coupling constant of the model D*** . In the Ehime case, CCE has no relevance since it is constructed in a single-channel approximation. In the FG-A case, however, CCE is significant, and is taken into account by adding an extra term $\Delta V_{\rm sim}(r)$ to the direct-channel part $V^D_{\Lambda\Lambda}(^1S_0)$ so that $V^{(\rm eff)}_{\Lambda\Lambda}(^1S_0) \equiv V^D_{\Lambda\Lambda}(^1S_0) + \Delta V_{\rm sim}(r)$ simulates the $^1S_0$ $\Lambda\Lambda$ phase shifts including CCE. In practice we use this $V^{(\rm eff)}_{\Lambda\Lambda}(^1S_0)$ as $V_{\Lambda\Lambda}(^1S_0)$ for the FG-A potential, by taking $\Delta V_{\rm sim}(r) = 93e^{-(r/r_1)^2} - 1000e^{-(r/r_2)^2}$ MeV with $r_1 = 1.0$ fm and $r_2 = 0.6$

*** The statement "this channel coupling effect, although small, is included similarly through the original t-matrix to be fitted" appeared in Ref. 22) (also similar statement in Refs. 2) and 3)) is inadequate and should be revised as above.

fm.

In Fig.4, phase shifts from three potentials are displayed as a function of $E_{YY}^{\rm lab}$. For $\Lambda\Lambda$, they give almost similar results at low $E_{YY}^{\rm lab}$ and the deviations among them develop with the inclease of $E_{YY}^{\rm lab}$ as a reflection of short-range behavior in the YY potentials. For the YY potentials, the experimental information exists only for the $\Lambda\Lambda$ case, i.e., the double Λ hypernuclei. ND-soft and Ehime have been checked to reproduce well the bond energy $\Delta B_{\Lambda\Lambda}(\simeq (4-5)$ MeV) for ${}^{10}_{\Lambda\Lambda}$Be and ${}^{13}_{\Lambda\Lambda}$B.[40)-44)] Also in FG-A, this reproduction is well expected since the phase shifts from FG-A are similar to those from ND-Soft and Ehime at low scattering energies. Recently, however, there arises the problem that $\Delta B_{\Lambda\Lambda} \simeq (4-5)$ MeV extracted from ${}^{10}_{\Lambda\Lambda}$Be and ${}^{13}_{\Lambda\Lambda}$B (old data) might be too large and instead $\Delta B_{\Lambda\Lambda} \sim 1$ MeV from ${}^{6}_{\Lambda\Lambda}$He ("NAGARA event"[45)], new data) should be the fact. This suggests that the $\Lambda\Lambda$ interaction is less attractive than that taken so far. If this is true, the realization of Y-superfluidity is affected so much. The discussion about this problem will be given in §5.

§4. Numerical results and discussion

4.1. *Realization of hyperon superfluidity*

First we discuss how the energy gap for hyperon pairing is realizable by referring to the well-known case of nucleon pairing. We focus our attention to the effects of pairing interactions and effective-mass parameters. For this purpose, the energy gaps Δ_i ($\equiv \Delta_i(q_{Fi})$; $i = \Lambda$ and p) calculated from a set of Eqs.(1)$\sim$(4) at $T = 0$, as functions of fractional density $\rho_i(\equiv y_i\rho)$, are compared in Fig.5, where the pairing interaction $V_{ii}({}^1S_0)$ is taken from the ND-Soft potential for $i = \Lambda$ and the OPEG ^{1}E-1 potential[46)] for $i = p$. We observe the following three points. First,the relation that Δ_p is larger for $M_p^* = 0.8M_\Lambda$ than for $M_p^* = 0.8M_p$ means that p-superfluid occurs more likely if bare mass of p is as large as that of Λ, conversely speaking, Λ-superfluid is realized more easily than p-superfluid due to $M_\Lambda > M_p$ for the same m_i^*, y_i and $V_{ii}({}^1S_0)$, as has been mentioned in §3. Second, comparison of Δ_p with Δ_Λ for the same effective-mass ($M_p^* = M_\Lambda^* = 0.8M_\Lambda$) and the same y_i shows that p-superfluidity is more likely to occur than Λ-superfluidity as far as the pairing interaction is concerned, which is reflected by stronger attraction of $V_{NN}({}^1S_0)$ as shown in Fig. 4(a). Third, for the same y_i, Δ_p for $M_p^* = 0.5M_p$ is smaller than Δ_Λ for $M_\Lambda^* = 0.8M_\Lambda$ in spite of stronger attraction of $V_{pp}({}^1S_0)$, which suggests that if actual $m_i^*(\rho)$ in medium (Fig.3) is taken account, i.e., the case of $m_\Lambda^* > 0.8$ compared to the case of $m_p^* \sim 0.5$ for $\rho \gtrsim 4\rho_0$, Δ_Λ would be much larger than Δ_p. In fact, as will be presented just below, we have Λ-superfluidity and also Σ^-- superfluidity in NS cores, but we have no p- superfluid because of a serious effect coming from very small $m_p^*(\rho)$ and relatively large ρ_p (namely y_p). Thus we can say that Y-superfluidity in dense NS cores occures due to the attractive effect of $V_{YY}({}^1S_0)$ not so different from $V_{NN}({}^1S_0)$ and mainly due to the strong aids from $m_Y^*(\rho)$ which is remarkably larger than $m_N^*(\rho)$.

Results for a realistic case with ρ-dependent m_Y^* and y_Y are shown in Fig.6

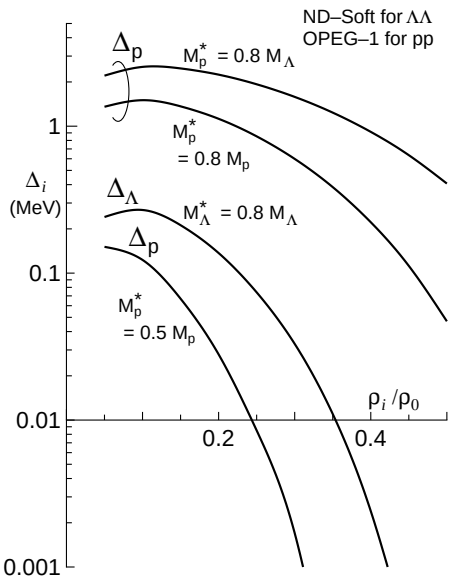

Fig. 5. Energy gaps Δ_i for proton ($i = p$) and Lambda ($i = \Lambda$) as a function of the fractional density $\rho_i (= y_i \rho)$, showing the effects of three factors, i.e., pairing interaction, effective mass M_i^* and fractional density $\rho_i (= y_i \rho)$ controling solutions of the energy gap equation, and serving to the understanding of a realization of Λ-superfluid. Pairing potential used for $\Lambda\Lambda$ (pp) pairing is ND-Soft (OPEG ^{1}E-1).

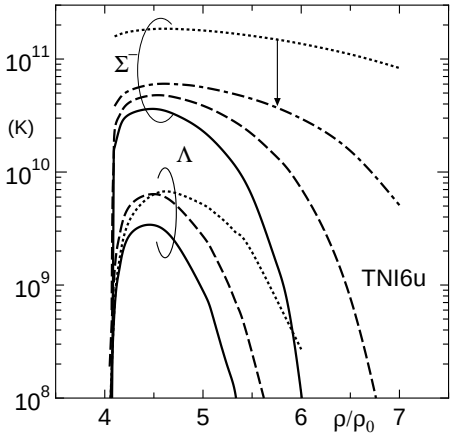

Fig. 6. Hyperon energy gap $\Delta_i (i = \Lambda, \Sigma^-)$ in Y-mixed NS matter, expressed in terms of the critical temperature $T_{ci}^* \simeq 0.57\Delta_i/\kappa_{\rm B}$ in Eq.(4.1), as a function of total baryon density ρ. The solid, dashed and dotted lines are for the ND-Soft, Ehime and FG-A potentials, respectively. An arrow indicates the reduction of $T_{c\Sigma^-}$ when the information of less attractive $\Lambda\Lambda$ interaction suggested by the "NAGARA event" ${}^{6}_{\Lambda\Lambda}$He is incorporated in the baryon-baryon interaction model with OBE and SU(3) symmetry frameworks. The reduction of Δ_Λ is serious and too small to be figured, i.e., $T_{c\Lambda}^* << 10^8$ K.

for TNI6u NS model as an example, in terms of a critical temperature T_{cY}^* for Y-superfluidity defined by

$$T_{cY}^* \equiv 0.57\Delta_Y/\kappa_{\rm B} \simeq 0.66\Delta_Y \times 10^{10} K \qquad (4{\cdot}1)$$

with Δ_Y in MeV calculated at $T = 0$ ($\Delta_Y \equiv \Delta_Y(q_F, T = 0)$). The solid, the dashed and the dotted lines correspond to the use of $Y_{YY}({}^1S_0)$ from the ND-Soft, the Ehime and the FG-A potentials, respectively. The Y-superfluidity occurs when T_{cY} exceeds $T_{in} \simeq 10^8$ K, the internal temperature of usual middle-aged NSs. Following points are noted:

(i) Both of Λ- and Σ^-- superfluids are likely to occur in NS cores since $T_{c\Lambda}$ and $T_{c\Sigma^-}$ are well above T_{in}. Λ and Σ^- become superfluids as soon as they appear in NS cores and Λ-superfluid is realized in a limited density region ($\rho \sim (4-6)\rho_0$) while Σ^--superfluid extends to much higher densities.

(ii) The aspects of T_{cY} versus ρ relationships for three different potentials are well bunched in the Λ case, as compared with those in the Σ^- case, which comes from less uncertainties of pairing interaction in the Λ case due to the check by double Λ

hypernuclei mentioned in §3.
(iii) $T_{c\Sigma^-}(\sim 10^{10-11}$ K) for Σ^--superfluid is larger than $T_{c\Lambda}(\sim 10^{9-10}$ K) for Λ-superfluid by more than one order of magnitude, which comes mainly from very large $m^*_{\Sigma^-}(\sim 1)$ compared to $m^*_\Lambda(\sim 0.8)$. The large $T_{c\Sigma^-}$ means that Σ^-- superfluidity is realizabe in NSs even at an early stage of the thermal evolution where T_{in} is as high as 10^{10} K.

Table III. Energy gaps Δ_Y of Λ and Σ^- in TNI6u Y-mixed NS matter at zero tempeeerature ($E = 0$) for several densities ρ and for three YY pairing interactions; ND-Soft, Ehime and FG-A. The mixing ratios y_Y and the effective-mass parameters $m^*_Y(\equiv M^*_Y/M_Y)$ of hyperons in medium are also given. Δ_Y at finite temperature ($T > 0$) is obtained by a profile function $P(\tau)$ given in §4.2.

Y	ρ/ρ_0	y_Y	m^*_Y	Δ_Y in MeV		
				ND-Soft	Ehime	FG-A
Λ	4.05	0.00057	0.818	0.006	0.019	0.006
	4.10	0.00225	0.820	0.061	0.133	0.067
	4.15	0.0046	0.821	0.140	0.274	0.168
	4.25	0.0102	0.825	0.274	0.496	0.370
	4.50	0.0261	0.832	0.339	0.638	0.635
	4.75	0.0422	0.839	0.219	0.486	0.641
	5.00	0.0578	0.845	0.089	0.271	0.516
	5.10	0.0638	0.847	0.053	0.196	0.450
	5.25	0.0726	0.850	0.019	0.106	0.348
	5.35	0.0782	0.852	0.008	0.065	0.285
	5.50	0.0865	0.854	0.001	0.025	0.195
	6.00	0.1116	0.860	0.	0.	0.027
Σ^-	4.10	0.00156	1.165	1.656	2.295	15.866
	4.15	0.0047	1.146	2.428	3.166	16.502
	4.25	0.0123	1.121	3.238	4.125	17.442
	4.50	0.0321	1.087	3.619	4.778	18.440
	4.75	0.0506	1.062	3.127	4.514	18.423
	5.00	0.0677	1.040	2.300	3.867	17.901
	5.25	0.0833	1.019	1.385	3.037	17.062
	5.50	0.0975	1.000	0.612	2.165	16.036
	5.75	0.1104	0.983	0.154	1.362	14.895
	6.00	0.1222	0.967	0.011	0.714	13.649
	6.50	0.1425	0.938	0.	0.077	11.010
	7.00	0.1591	0.914	0.	0.000	8.326

Full results of hyperon energy gaps for TNI6u NS models and for three $V_{YY}(^1S_0)$ are presented in Table III at several densities, together with the ρ-dependent input parameters, y_Y and m^*_Y, controling the solution of the energy gap equations (3·1)$\sim$ (3·4). In the cases of TNI3u and TNI2u, the points (i)$\sim$(iii) noted just above are very similar to TNI6u case. Thus we can say that Λ and Σ^- admixed in NS cores are surely in the superfluid state, although somewhat depending on the NS model and considerably on the pairing interaction $V_{YY}(^1S_0)$. The aspect of EOS-dependence of hyperon gap is shown in Fig.7.

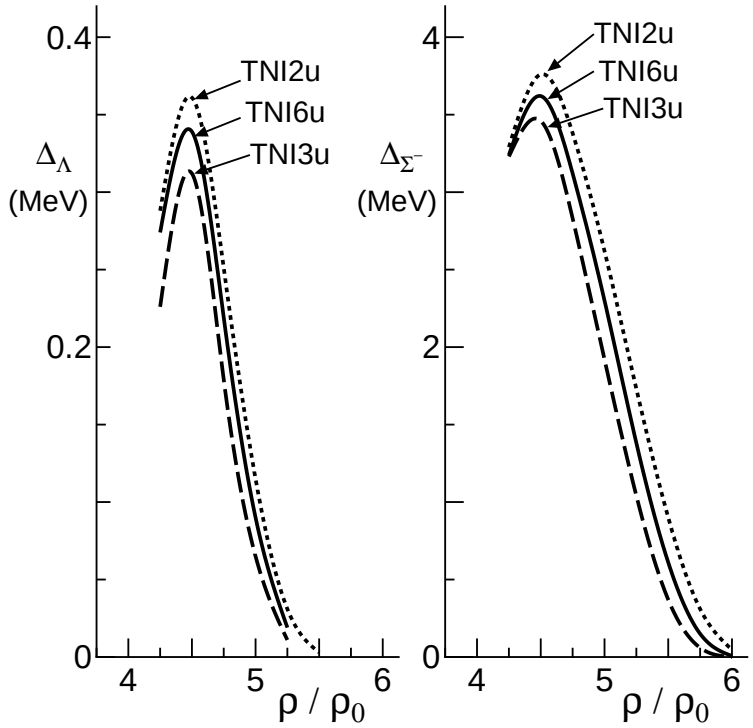

Fig. 7. Hyperon energy gap Δ_Y for ND-Soft pairing potential as a function of ρ for TNI2u, TNI6u and TNI3u EOSs, showing the extent of EOS dpendence of Δ_Y. Left-hand (Right-hand) side is for $\Lambda(\Sigma^-)$ case.

4.2. *Effects of finite temperature*

So far we have discussed the energy gaps at zero temperature. In cooling calculations of NSs, however, we need to take account of the temperture effects on the energy gaps, since the temperature T of Y- mixed NS matter varies according to the thermal evolution and in general the resulting energy gap Δ_Y decreases with increasing T.[47] The T-dependent energy gaps $\Delta_Y(T)$, the solution of the finite-temperature gap equations (3·1)∼(3·4), are shown in Fig.8 for a typical case with ND-Soft and TNI6u. We observe that Δ_Y depends remarkably on T, especially for small Δ_Y. In cooling calculations, it is of practical use to have a profile function $P(\tau)$ approximating the T-dependence of Δ_Y. According to our previous work,[48] we introduce $P(\tau)$ as a function of the argument τ defined by $\tau = T/T_c$:

$$P_Y(\tau) \equiv \Delta_Y(q_{FY}, T)/\Delta_Y(q_{FY}, T=0), \tag{4·2}$$

$$= 1 - \sqrt{2\pi a_0 \tau}\exp\left[-1/(a_0\tau)\right](1 + \alpha_1\tau + \alpha_2\tau^2) \quad (0 \le \tau \le \tau_b), \tag{4·3}$$

$$= a_0 C_1 \sqrt{1-\tau}[1 + \beta_1(1-\tau) + \beta_2(1-\tau)^2] \quad (\tau_b \le \tau \le 1), \tag{4·4}$$

$$a_0 = a_0^*(T_c/T_c^*) \tag{4·5}$$

where a_0, C_1, α_1, α_2, β_1 and β_2 are the constant parameters and $a_0^* = 0.57$ is given

Table IV. Parameters for profile function $P(\tau)$ ($\equiv \Delta_Y(T)/\Delta_Y(0)$) representing analytically the temperature dependence of hyperon(Y) energy gap.

Y	C_1	α_1	α_2	β_1	β_2
Λ	2.8963	-0.45902	1.41171	-0.13926	-0.53396
Σ^-	2.8504	-0.39488	1.38328	-0.09447	-0.57033

by the coefficient appearing in the definition of T_c^* in Eq.(4·1). Here $T_c(T_c^*)$ denotes real (approximate) critical temperature. Eq.(4·3) assures that the energy gap ratio (Eq.(4·2)) decreases from $P(\tau) = 1$ as T starts from $T = 0$ and Eq.(4·4) assures that $P(\tau) = 0$ at $T = T_c$.

From numerical calculations to search T_c, it is found that T_c is well substituted by T_c^*, except the case of Σ^- with FG-A potential where, due to particularly large Δ_{Σ^-}, $T_c \simeq (0.278{+}0.130(\rho/\rho_0))\times T_0^*$ at densities $(4{-}6)\rho_0$. By selecting the boundary value of two regions τ_b as $\tau_b = 0.7$ and fitting $\Delta(q_{FY},\ T = 0)P(\tau)$ to $\Delta(q_{FY},\ T)$ actually calculated, we have the parameters of $P(\tau)$ as in Table IV (details of the procedure are referred to Ref. 48)). The aspect of reproduction of $\Delta(q_{FY}, T)/\Delta(q_{FY},\ T = 0)$ by $P(\tau)$ is illustrated in Fig.9 for Λ as an example. Once $P(\tau)$ is obtained,

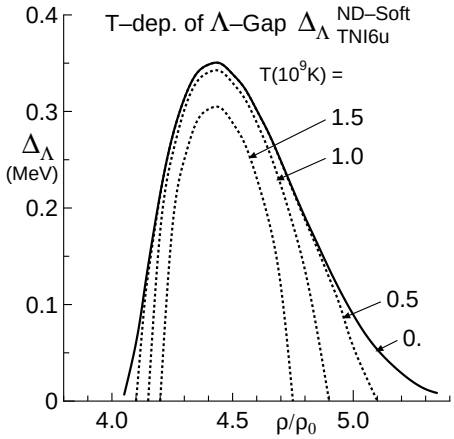

Fig. 8. Temperature(T) dependence of Λ energy gap (Δ_Λ) for the case of TNI6u EOS and ND-Soft potential, as an example.

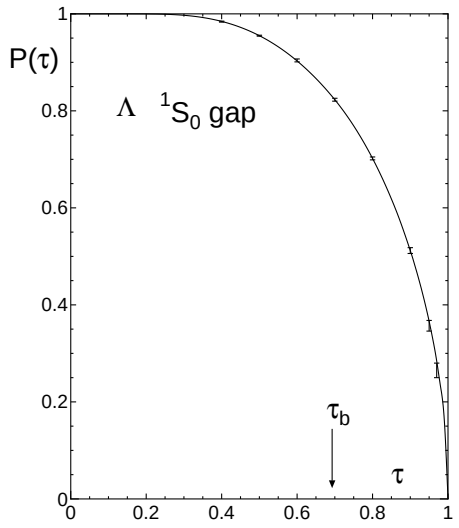

Fig. 9. Profile function $P_\Lambda(\tau)(\equiv \Delta_\Lambda(T)/\Delta_\Lambda(0))$ in the form of Eqs.(4.3) and (4.4) as a function of $\tau(\equiv T/T_{c\Lambda})$, averaged over the pairing potentials employed and the densities under consideration ($\rho \simeq (4-5)\rho_0$). Crosses and error bars denote the values obtained by numerical calculations of finite-temperature gap equation. $\tau_b = 0.7$ denotes the boundary between Eq.(4.3) region and Eq. (4.4) one. Parameters for $P_Y(\tau)(Y = \Lambda$ and $\Sigma^-)$ are listed in Table IV.

we can use an analytic form of T-dependent energy gap in NS cooling calculations, by utilizing the zero temperature gap $\Delta_Y(q_{FY}, T = 0)$.

4.3. *Momentum triangle condition for Y-DUrca cooling*

The ν-emission process responsible for NS cooling is operative only when a certain condition, namely, the so-called "momentum triangle condition" relevant to the momentum conservation in the corresponding reaction is satisfied. For example, a familiar β-decay process associated with nucleons (N) and its inverse process (called N-DUrca), i.e., $p \to n + l + \bar{\nu}_l$, $n + l \to p + \nu_l$ (abbreviated to as $p \leftrightarrow nl$ hereafter) is allowed when the Fermi momenta $k_i = q_{Fi} (= (3\pi^2 y_i \rho)^{1/3})$ for particles participating the reaction satisfy the triangle condition,

$$| k_p - k_l | < k_n < k_p + k_l \tag{4·6}$$

Here the Fermi momentum $k_\nu (\simeq \kappa_{\rm B} T/\hbar c)$ for neutrinos is neglected because it is much smaller than those of N and l. As well known, N-DUrca is forbidden in usual neutron star matter including n, p, e^- abd μ^- components, because the second inequality in Eq. (4·6) is hard to hold among n (large component, $y_n \gtrsim 0.9$), p (small component, $y_p \lesssim 0.1$) and l (small component, $y_l \lesssim 0.1$). Then, to satisfy the condition, it is necessary for another particle to participate as a bystander mediating momentum conservation and the ν-emission due to the modified Urca process ($pN \leftrightarrow nNl$) including a bystander nucleon becomes a main agency for the cooling of usual NSs, although the ν-emissibity is greatly reduced compared to the N-DUrca. In the case of normal NS matter ($npe^-\nu^-$ matter), the fast cooling due to N-DUrca is made possible only for NS models including high proton fraction phase with $y_p > 0.148$. [49)]

How about the situation in the Y-mixed NS matter ($np\Lambda\Sigma^- e^- \mu^-$ matter) under consideration ? In Fig.10, the triangle condition is checked for DUrca processes, i.e., N-DUrca and Y-DUrca, for the Y-mixed NS matter of TNI6u EOS by using the fractions y_i in Table II(b). The aspects for other EOS, TNI2u EOS (Table II(a)) and TNI3u EOS (Table II(c)), are very similar to those in Fig.10. We note the following points:

(i) In the Y-mixed phase, the proton fraction y_p becomes remarkablely larger than that of usual NS matter ($npe^-\mu^-$ matter), increasing with ρ and reaching up to 20% at $\rho \sim 8\rho_0$. But Fig.10 shows that N-DUrca is not operative up to high density region, i.e., $\rho \lesssim 6.5\rho_0$ for $n \leftrightarrow pe^-$ and $\rho \lesssim 8\rho_0$ for $n \leftrightarrow p\mu^-$. Combining the M-ρ_c relationship in Fig.2, this means that N-DUrca cooling begins to operate only for rather massive NSs with $M \gtrsim 1.6 M_\odot$ for $n \leftrightarrow pe^-$ DUrca and $M \gtrsim 1.7 M_\odot$ for $n \leftrightarrow p\mu^-$ DUrca.

(ii) In contrast with N-DUrca mentioned above, the Y-DUrca of $\Lambda \leftrightarrow pl$ type can operate as soon as Λ begins to appear, i.e., $\rho \gtrsim 4\rho_0$ both for $l \equiv e^-$ and $l \equiv \mu^-$. This is because the triangle condition is easy to be satisfied due to the fact that all the particles participating the reactions are of small components, not including the large n-component. From Fig.2, we see that $\Lambda \leftrightarrow pl$ Y-DUrca can work in all the

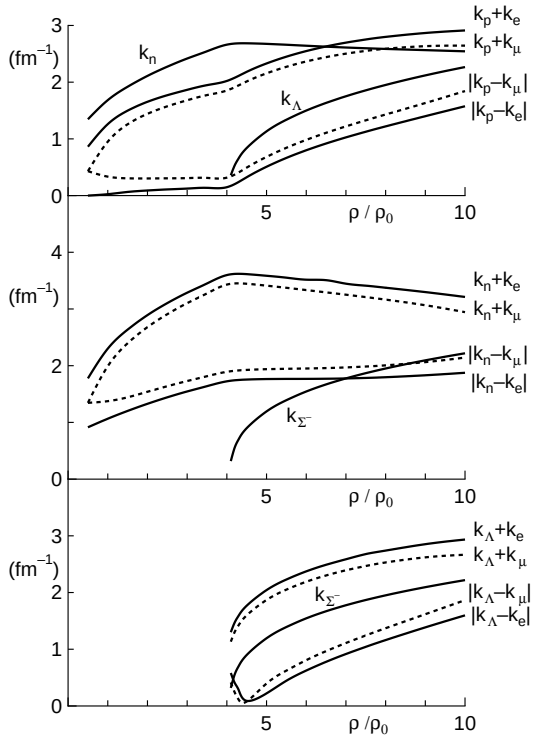

Fig. 10. Momentum triangle condition to check the operation of various DUrca ν-emission processes in the text, where $k_i = q_{Fi}(= (3\pi^2 y_i \rho)^{1/3})$ is the Fermi momentum of respctive constituent ($i = n$, p, Λ, e^-, μ^-), in Y-mixed NS matter with TNI6u EOS; upper panel is for $n \leftrightarrow p + l$ process, middle panel is for $\Sigma^- \leftrightarrow n + l$, and lower one is for $\Sigma^- \leftrightarrow \Lambda + l$ process, depending on ρ. Solid (dotted) lines are for the case with $l = e^-$ (μ^-).

Y-Mixed NSs with $M \gtrsim 1.35 M_\odot$ and provides a very fast cooling of NSs.
(iii) The Y-DUrca of $\Sigma^- \leftrightarrow nl$ type including the large n-component is hard to be operative. It is impossible for NSs with the central density $\rho_c \lesssim 7\rho_0$ for $\Sigma^- \leftrightarrow ne^-$ and $\rho_c \lesssim 8.5\rho_0$ for $\Sigma^- \leftrightarrow n\mu^-$; this means that $\Sigma^- \leftrightarrow nl$ Y-DUrca occurs only for NS with $M > 1.6 M_\odot$ for $l \equiv e^-$ case and $M > 1.7 M_\odot$ for $l \equiv \mu^-$. On the other hand, like $\Lambda \to pl$ type, the Y-DUrca of $\Sigma^- \leftrightarrow \Lambda l$ type occurs as soon as Σ^- appears because all the associated particles are small components. It should be noticed, however, that the Y-DUrca including Σ^- is made possible only for the density region where Λ coexists with Σ^-. That is, the particlipation of Λ in NS constituents is essential for the Y-DUrca to operate.

Based on (i)$\sim$(iii), it is remarked that the momentum triangle condition interestingly limits the density region (in other words, NS mass) and the type of DUrca processes. Except for massive NS stars, the Λ mixing is a main agency for Y-DUrca cooling.

4.4. *Superfluid suppression effects on neutrino-emissivities*

As mentioned in §1, solely the fast cooling due to Y-DUrca operation is not satisfactory for the explanation of colder class NSs, because its extremely efficient ν-emission causes a serious problem of too rapid cooling. Here we discuss the suppression effects on ν- emissivities due to the nucleon and hyperon superfluidities, by using the energy gaps in Table II and their T-dependence given by the profile function $P(\tau)$ in §4.2. The Y-DUrca ν-emissivities, $\epsilon_{\rm DU}(\Lambda \leftrightarrow p) \equiv \epsilon_{\rm DU}(\Lambda \leftrightarrow pe^-) + (\Lambda \leftrightarrow p\mu^-)$ and $\epsilon_{\rm DU}(\Sigma^- \leftrightarrow \Lambda) \equiv \epsilon_{\rm DU}(\Sigma^- \leftrightarrow \Lambda e^-) + \epsilon_{\rm DU}(\Sigma^- \leftrightarrow \Lambda\mu^-)$, are given by

$$\epsilon_{\rm DU}(\Lambda \leftrightarrow p) = 0.158 \times 10^{21} T_8^6 (y_e \rho/\rho_0)^{1/3} \times m_\Lambda^* m_p^* (M_\Lambda M_p/M_n^2) R_{AA}(\Lambda, p)(\theta_e + \theta_\mu) \quad (4\cdot7)$$

$$\epsilon_{\rm DU}(\Sigma^- \leftrightarrow \Lambda) = 0.822 \times 10^{21} T_8^6 (y_e \rho/\rho_0)^{1/3} \times m_{\Sigma^-}^* m_\Lambda^* (M_{\Sigma^-} M_\Lambda/M_n^2) R_{AA}(\Sigma^-, \Lambda)(\theta_e + \theta_\mu) \quad (4\cdot8)$$

where $T_8 \equiv T/10^8$ K, $\theta_l = 1(0)$ for the process allowed (not allowed) and $R_{AA}(B_1,$ $B_2)$ is the superfluid suppression factor relevant to participating baryons B_1 and B_2. The appearance of y_e comes from the chemical equilibrium; $\mu_e = \mu_\mu \simeq \hbar q_{Fe} c$. $R_{AA}(B_1,\ B_2)$ is defined by the ratio of the integral of statistical factors in the $^1S_0$ superfluid phase (I_s) to that in the normal phase (I_0), i.e., $R_{AA}(B_1,\ B_2) \equiv I_s/I_0$, which represents the decrease of the number density around the Fermi surface due to the energy gap (more details including calculational methods are referred to Ref. 48)).

Calculated results are shown in Fig. 11 for TNI6u EOS and energy gaps from ND-Soft pairing potential. Fig.11(a) demonstrates the suppression effects $R_{AA}(B_1,$ $B_2)$ as a function of ρ by taking two typical NS temperatures, $T = 1 \times 10^8$ K and 5×10^8 K. $R_{AA}(B_1,\ B_2)$ depends strongly on both ρ and T, reflected by the ρ- and T- dependent energy gaps of B_1 and B_2. For example, $R_{AA}(\Lambda,\ p)$ for $\Lambda \leftrightarrow p$ process (solid lines) depends on ρ as $R_{AA} \simeq 1 \to 10^{-1} \to 1$ for $\rho/\rho_0 \simeq 4 \to 4.5 \to 5.0$ at $T = 5 \times 10^8$ K. When the temperature dectreases to $T = 1 \times 10^8$ K, the suppression works by far stronger; $R_{AA} \simeq 1 \to 10^{-11.5} \to 1$. Apart from the details, this characteric feature is qualititively understood by an exponential damping factor, $\exp[-(\Delta_{B_1} + \Delta_{B_2})/\kappa_B T]$ involved in $R_{AA}(B_1,\ B_2)$, together with the ρ- and T-dependences of Δ_{B_1} and Δ_{B_2} in Fig. 6 (in $\Lambda \leftrightarrow p$ process, $\Delta_p = 0$ as mentioned in §4.1.). For $\Sigma^- \leftrightarrow \Lambda$ process, the ρ- and T- dependent aspect of $R_{AA}(\Sigma^-,\ \Lambda)$ is extremely enlarged because of large energy gaps of Σ^-.

Fig.11(b) illustrates how emissivities $\epsilon_{\rm DU}(B_1 \leftrightarrow B_2)$ for Y-DUrca are moderated by $R_{AA}(B_1,\ B_2)$, where emissivities ϵ_{MD} for the modified Urca including superfluid suppression (see Ref. 48) for details) are also shown for comparison. First we consider $\epsilon(\Lambda \leftrightarrow p)$ (solid lines) in the density range $\rho \simeq (4-5)\rho_0$. At $T = 5 \times 10^8$ K, the effect of $R_{AA}(\Lambda,\ p)$ is not remarkable and $\epsilon_{\rm DU}(\Lambda \leftrightarrow p) \sim 10^{23-24}$ erg/cm^{3}s is much larger than $\epsilon_{\rm MU} \sim 10^{18-19}$ erg/cm^{3}s. On the other hand, at $T = 1 \times 10^8$ K, the situation is changed remarkably; $\epsilon_{\rm DU}(\Lambda \leftrightarrow p) \sim 10^{20}$ erg/cm^{3}s for no suppression (dash-dotted lines) is maximumly suppressed to $\epsilon_{\rm DU}(\Lambda \leftrightarrow p) \sim 10^{8.5}$ erg/cm^{3}s by $R_{AA}(\Lambda,\ p)$ and even smaller than $\epsilon_{\rm MU} \sim 10^{12-13}$ erg/cm^{3}s for $\rho \sim (4.2 - 4.7)\rho_0$, although $\epsilon_{\rm DU}(\Lambda \leftrightarrow p) \gtrsim \epsilon_{MU}$ persists for other densities. The behavior of $\epsilon_{\rm DU}(\Lambda \leftrightarrow p)$ for

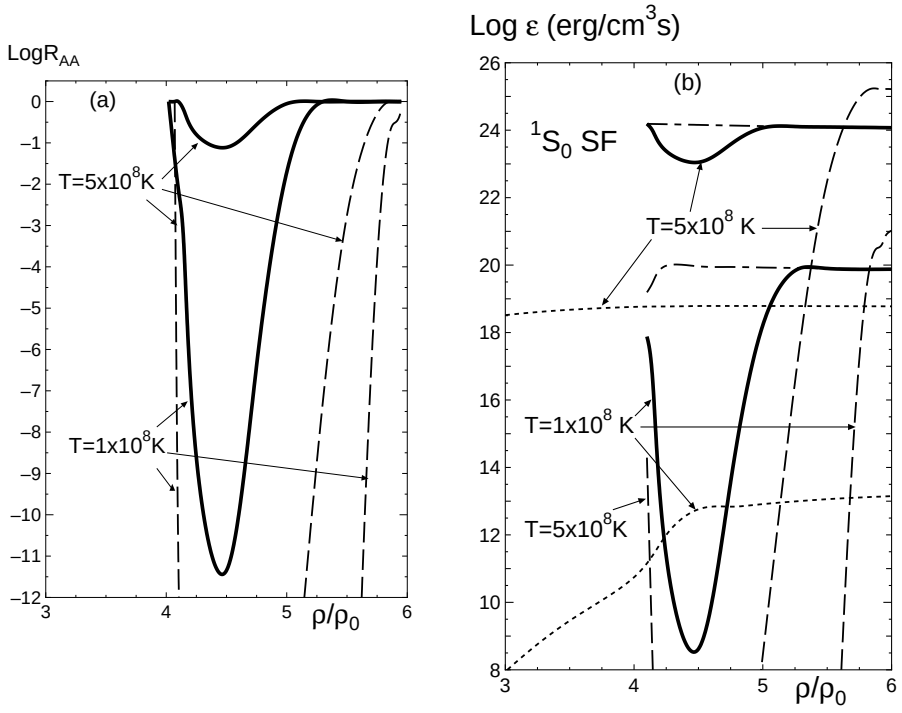

Fig. 11. (a) Superfluid suppression factor $R_{\Lambda\Lambda}(B_1,\ B_2)$ on ν-emissivity relevant to baryons (B_1, B_2) participating in the Y-DUrca processes, as functions of ρ and for two typical temperatures of NS interior, $T = 1 \times 10^8$ K and 5×10^8 K. Solid lines (dashed lines) is for $\Lambda \leftrightarrow p$. ($\Sigma^- \leftrightarrow \Lambda$) process summed over $\Lambda \leftrightarrow p + e^-$ and $\Lambda \leftrightarrow p + \mu^-$($\Sigma^- \leftrightarrow \Lambda + e^-$ and $\Sigma^- \leftrightarrow \Lambda + \mu^-$). (b) Y-DUrca ν-emissibity including the superfluid suppression effect corresponding to $R_{\Lambda\Lambda}(B_1,\ B_2)$ in (a), as functions of ρ and two typical temperatures. Solid lines (dashed lines) is for Y-DUrca of $\Lambda \leftrightarrow p(\Sigma^- \leftrightarrow \Lambda)$ type and dotted lines are for the modified Urca processes responsible for the standard cooling of NSs. As an example, the emissivities without the superfluid suppression are also shown by dash-dotted lines in the case of $\Lambda \leftrightarrow p$ process, for reference.

$T = 5 \times 10^8$ K $\rightarrow 1 \times 10^8$ K tells us that at higher T in relatively earlier stage of thermal evolution, the $\Lambda \leftrightarrow p$ process dramatically accelerates the NS cooling as compared to the standard modified Urca process, but this acceleration undergoes a braking effect due to superfluid suppression with decreasing T in later stage, avoiding too rapid cooling. In the case of $\Sigma^- \leftrightarrow \Lambda$ process, $\epsilon_{\rm DU}(\Sigma^- \leftrightarrow \Lambda)$ is much smaller than $\epsilon_{\rm MU}$ as well as $\epsilon_{\rm DU}(\Lambda \leftrightarrow p)$ for $\rho \sim (4-5)\rho_0$, due to extremely strong suppression of $R_{AA}(\Sigma^-,\ \Lambda)$. In the total ν-emissivity, the most efficient ν-emission process is of prime importance. So $\Sigma^- \leftrightarrow \Lambda$ process becomes appreciable only at high densities ($\rho \gtrsim 5.5\rho_0$) where $\epsilon_{\rm DU}(\Sigma^- \leftrightarrow \Lambda)$ becomes comparable or larger compared to $\epsilon_{\rm DU}(\Lambda \leftrightarrow p)$ depending on T. At high densities ($\rho > 5\rho_0$), $\epsilon_{\rm DU}(\Lambda \leftrightarrow p)$ and /or $\epsilon_{\rm DU}(\Sigma^- \leftrightarrow \Lambda)$ suffer no suppression because of disappearance of superfluidities and hence massive NSs with $\rho_c > 5\rho_0$ cause a problem of too rapid cooling. This negative situation is quite the same for the N-DUrca cooling mentioned in §4.1 which becomes possible at $\rho \gtrsim 6.5\rho_0$, because the n and p superfluidities completely disappear at these high densities.

Bearing two conditions, i.e., the triangle condition to allow fast DUrca cooling and the superfluid suppression condition to moderate the cooling rate (avoiding too rapid cooling), we can say that the Y-DUrca of $\Lambda \leftrightarrow p$ type plays a decicive role to generate cooling scenario for colder class NSs. [48] This is because firstly $\Sigma^- \leftrightarrow \Lambda$ process can work only under the coexistence of Λ and secondary the large Σ^- gap suppresses $\epsilon_{\rm DU}(\Sigma^- \leftrightarrow \Lambda)$ too strongly . To be consistent with surface temperature observations of NSs, we can constrain the mass of colder class NSs as follows. For the TNI6u NS models, it must be larger than about $1.35M_\odot$ in order to give $\rho_c > \rho_t(Y)$ and also be smaller than about $1.55M_\odot$ in order to avoid too rapid cooling. Of course this mass restriction depends on the NS model (Fig.2) and superfluid gap Δ (Fig.6), but anyway the operation of the Y-DUrca moderated by the baryon superfluidity provides us with a new idea for NS cooling. That is, less massive NSs (hence no Y-mixed core) cooled slowly by the standard process (modified Urca) correspond to hotter class NSs and massive NSs (with Y-mixed core and superfluids) cooled rapidly by the nonstandard process (Y-DUrca) correspond to colder class NSs. In fact, cooling calculations, though preliminary, nicely explain the surface temperature observations by this idea. [10]

§5. Less attractive $\Lambda\Lambda$ interaction

We have discussed that the hyperon cooling scenario for NSs is consistent with observations and the occurrence of Λ-superfluidity is of particular importance. There exists, however, an experimental information contradicting the occurrence. Recently the KEK-E373 group observed one event of the Λ hypernucleus ${}^{6}_{\Lambda\Lambda}$He in the emulsion experiment, called "NAGARA event" and extracted new information of $\Delta B_{\Lambda\Lambda} \simeq 1$ MeV for the $\Lambda\Lambda$ bond energy from a difference of binding energy B between double and single Λ hypernuclei, [45]

$$\Delta B_{\Lambda\Lambda} = B({}^{6}_{\Lambda\Lambda}\mathrm{He}) - 2 \times B({}^{5}_{\Lambda}\mathrm{He}). \qquad (5\cdot1)$$

This new result of $\Delta B_{\Lambda\Lambda} \simeq 1$ MeV is much smaller than the old $\Delta B_{\Lambda\Lambda} \simeq (4-5)$ MeV extracted from ${}^{10}_{\Lambda\Lambda}Be$ and ${}^{13}_{\Lambda\Lambda}B$, suggesting that the $\Lambda\Lambda$ attraction responsible for Λ-superfluidity would be much weaker than that taken so far. Since all the pairing interacations, ND-Soft, Ehime and FG-A, used in the present calculations of Λ-gap (§3) are taken to be consistent with old $\Delta B_{\Lambda\Lambda} \simeq (4-5)$ MeV, the new finding of $\Delta B_{\Lambda\Lambda} \simeq 1$ MeV is serious and necessitates a reexamination of Λ-gaps for the reduced $\Lambda\Lambda$ attraction. Hiyama et al., [50] by performing the energy calculations for $\alpha + \Lambda + \Lambda$ system, found that $\Delta B_{\Lambda\Lambda} \simeq 1$ MeV is reproduced by taking $V^{\rm ND}_{\Lambda\Lambda}({}^1S_0) \to \tilde{V}^{\rm ND}_{\Lambda\Lambda}({}^1S_0) \simeq 0.5 V^{\rm ND}_{\Lambda\Lambda}({}^1S_0)$. Precisely speaking, the potential strength in the modified ND-Soft $\tilde{V}^{\rm ND}_{\Lambda\Lambda}({}^1S_0)$ is multiplied by a factor 0.45 for the shortest-range term and a factor 0.5 for the intermediate- and long-range terms. By using this $\tilde{V}^{\rm ND}_{\Lambda\Lambda}({}^1S_0)$, we have tried to calculate Δ_Λ and found that the Λ-superfluidity does not occur, i.e., $T_c(\Lambda) << T_{in} \simeq 10^8$ K. Then we have a question how about Δ_{Σ^-} since YY interactions are internally related from the view of OBE plus SU(3) symmetry hypothesis. To see this, we reconstruct the BB interaction model of FG-A

so as to reproduce the $\Lambda\Lambda$ phase shifts from $\tilde{V}^{\rm ND}_{\Lambda\Lambda}(^1S_0)$, by weakening the attractive contribution form the σ-meson exchange. Through new parameters adjusted, new $\Sigma^-\Sigma^-$ interaction $\tilde{V}^{\rm FG}_{\Sigma^-\Sigma^-}$ is to be obtained. This can be done as follows. [51)]

In the framework of octet baryons plus nonet mesons with SU(3) symmetry, the coupling constants $\tilde{g}_{BBm} = g_{BBm}/\sqrt{4\pi}$ for the BB interaction by single meson (m) exchange are given in terms of 4 parameters, i.e., singlet coupling $\tilde{g}^{(0)}$, octet coupling $\tilde{g}^{(8)}$, parameter α relevant to a so-called F-D ratio, and mixing angle θ. Therefore a set of these 4 parameters are uniquely determined when 4 coupling constants are given. Here we pay our attention to the condition not to influence the NN interaction sector since it is well determined. So we use, as 4 coupling constant, $\tilde{g}_{NN\sigma}$, $\tilde{g}_{NNa_0}$, $\tilde{g}_{NNf_0}$ which are unchanged from the original FG-A model, and $\tilde{g}_{\Lambda\Lambda\sigma}$ which is adjusted so as to reproduce the phase shifts form $\tilde{V}^{\rm ND}_{\Lambda\Lambda}(^1S_0)$ compatible with the information from ${}^{6}_{\Lambda\Lambda}$He:

$$\tilde{g}_{NN\sigma} = \tilde{g}^{(0)}\cos\theta + (4\alpha-1)/\sqrt{3}\cdot\tilde{g}^{(8)}\sin\theta, \quad (5\cdot2a)$$

$$\tilde{g}_{NNa_0} = \tilde{g}^{(8)} \quad (5\cdot2b)$$

$$\tilde{g}_{NNf_0} = (4\alpha-1)/\sqrt{3}\cdot\tilde{g}^{(8)}\cos\theta - \tilde{g}^{(1)}\sin\theta, \quad (5\cdot2c)$$

$$\tilde{g}_{\Lambda\Lambda\sigma} = \tilde{g}^{(1)}\cos\theta - 2(1-\alpha)/\sqrt{3}\cdot\tilde{g}^{(8)}\sin\theta. \quad (5\cdot2d)$$

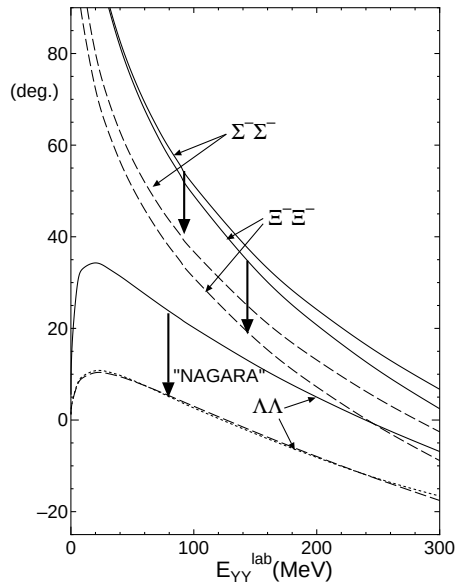

Fig. 12. Aspects to show how the attractive features of ${}^1S_0$ YY interactions (Fig.4) are weakened by taking account of less attractive $\Lambda\Lambda$ interaction suggested by the "NAGARA event" ${}^{6}_{\Lambda\Lambda}He$ in the frame work of OBE plus SU(3) symmtry. Solid lines (dashed lines) are ${}^1S_0$ phase shifts for the original FG-A potential $V^{\rm FG}_{YY}$ (the modified FG-A potential $\tilde{V}^{\rm FG}_{YY}$). The modification ($V^{\rm FG}_{YY} \to \tilde{V}^{\rm FG}_{YY}$) has been done through the fitting of $\tilde{V}^{\rm FG}_{\Lambda\Lambda}$ to $\tilde{V}^{\rm ND}_{\Lambda\Lambda}$ obtained by the reproduction of $\Lambda\Lambda$ bond energy of ${}^{6}_{\Lambda\Lambda}$He and the phase shifts from $\tilde{V}^{\rm ND}_{\Lambda\Lambda}$ are shown by the dotted line for reference.

Actually, about 10% reduction of $\tilde{g}_{\Lambda\Lambda\sigma}$ is satisfactory for the reproduction of the phase shifts at low scattering energies ($\lesssim 50$ MeV) corresponding to the pairing problem of Λ. From a new set of $\{\tilde{g}^{(1)},\ \tilde{g}^{(s)},\ \alpha,\ \theta\}$, new $\tilde{g}_{\Lambda\Lambda m}$ and $\tilde{g}_{\Sigma^-\Sigma^- m}$ responsible for the modified $\tilde{V}^{\rm FG}_{\Lambda\Lambda}({}^1S_0)$ and $\tilde{V}^{\rm FG}_{\Sigma^-\Sigma^-}({}^1S_0)$ are obtained as in Table V. Fig.12 compares the attractive effects between $V^{\rm FG}_{YY}({}^1S_0)$ (solid lines) and $\tilde{V}^{\rm FG}_{YY}({}^1S_0)$ (dashed lines) in terms of their phase shifts. We see that the $\Sigma^-\Sigma^-$ attraction of modified FG-A, as well as $\Lambda\Lambda$ case, is remarkably reduced from that of original FG-A. However, $\tilde{V}^{\rm FG}_{\Sigma^-\Sigma^-}({}^1S_0)$ remains to be more attractive than original $V^{\rm ND}_{\Lambda\Lambda}({}^1S_0)$, implying the persistence of Σ^--superfluidity. In fact, the reexamination of Δ_{Σ^-} with $\tilde{V}^{\rm FG}_{\Sigma^-\Sigma^-}({}^1S_0)$ shows that the Σ^--superfluid is realized with the $T_c(\Sigma^-)$ reduced by about a half, as indicated by an arrow in Fig.6. By the way, Fig.12 shows that the situation for $\Xi^-\Xi^-$ case is similar to the $\Sigma^-\Sigma^-$ case, suggesting that Ξ^- when admixed in NS cores could be in the superfluid state.

To summarize, the less attractive $\Lambda\Lambda$ interaction suggested by the NAGARA event leads to the disappearance of Λ-superfluid, although Σ^- superfluids can persist, and the Y-cooling scenario is faced to a serious problem of too rapid cooling by missing the superfluid suppression on the ν-emissibity for the $\Lambda \leftrightarrow pl$ process.

Table V. Coupling constant $\tilde{g}_{YYm}$ for modified FG-A potential($\tilde{V}^{FG}_{YY}$) to take account of "NAGARA event" information. Numbers in parenthesis are for original FG-A potential(V^{FG}_{YY}).

$\tilde{g}_{YYm}\backslash m$	σ	f_0	a_0
$\tilde{g}_{\Lambda\Lambda m}$	4.656	2.0849	0
	(5.15543)	(2.46243)	(0)
$\tilde{g}_{\Sigma^-\Sigma^- m}$	4.4265	-2.5360	5.5307
	(5.53592)	(-1.41267)	(4.89611)
$\tilde{g}_{\Xi^-\Xi^- m}$	4.3610	-3.8542	4.7687
	(5.66490)	(-2.72596)	(4.13408)

§6. Summary and remarks

We have calculated the energy gaps of Λ and Σ^- admixed in NS cores, for the mixing ratios and effective mass parameters of the Y-mixed NS models obtained realistically by the G-matrix-based effective interaction approach, and by adopting several pairing potentials to cover the uncertainties of YY interactions. It is found that both of Λ- and Σ^-- superfluids are realized as soon as they begin to appear at around $4\rho_0$, although the magnitude of critical temperature and maximum density for existence of the gaps depend considerably on the pairing potential. The EOSs for Y-mixed NS matter with different stiffness, together with the fractions of respective components, and also Λ- and Σ^-- energy gaps are numerically tabulated. The profile function $P(\tau)$ is presented to give analytically the temperature dependence of energy gaps. The presentation of these physical quantities serves as physical inputs for the calculations of Y- cooling for NSs.

Occurrence of Y superfluidity is vital for the Y-cooling scenario to be consistent with observations of colder class NSs, since otherwise enormous ν-emissivities due to Y-DUrca processes are not moderated by the superfluid suppression effects and cause

a serious problem of too rapid cooling generally encountered in DUrca processes. The momenturm triangle conditions to discriminate the operative DUrca processes are checked in Y-mixed NS matter. By combining the effects of superfluid suppression, it is found that in the Y-DUrca processes only the $\Lambda \leftrightarrow pl$ and $\Sigma^- \leftrightarrow \Lambda l$ processes can operate, and the former plays a decicive role in the Y-cooling whereas the latter is completely supressed due to the large Σ^- gaps except for particulary dense core of NSs. The N-DUrca currently taken is excluded for fast cooling scenario because it does not take place in core densities of medium mass NSs and its operation in massive NSs encounters the problem of too rapid cooling owing to a complete disappearance of nucleon energy gaps. On the basis of investigations presented here, we can say that the Y-cooling scenario combined with the Y-superfluidity, is a promising candidate for nonstandard fast cooling of NSs. The scenario can explain observations in the way that hotter class NSs has lighter masses (e.g., $M \lesssim 1.35 M_\odot$ for TNI6u plus ND-Soft and no Y-mixed core) are cooled slowly by the standard modified Urca, on the other hand, colder class NSs have medium masses ($M \sim (1.4 - 1.5) M_\odot$ with Y-superfluids) and are cooled rapidly by a moderated nonstandered cooling of Y-DUrca. The massive NSs ($M \gtrsim 1.55 M_\odot$) including dense core with disappearance of Y-superfluids causes too rapid cooling and are excluded if an extremely cooled NSs are not found. It is worth noting that observations of surface temperature limit interestingly the mass of NSs.

Less attractive $\Lambda\Lambda$ interaction inferred from the NAGARA event ${}^{6}_{\Lambda\Lambda}$He affects so much the Y-cooling scenario. It is shown that the Λ-superfluidity disappears when this less attraction is taken into account although the Σ^--superfluidity survives. This leads to the fact that the Y-cooling scenario, where the Λ-superfluid plays an essential role, breaks down due to the too rapid cooling. The decisive concludion, however, has to be postponed until the less attractive $\Lambda\Lambda$ interaction not to allow the Λ-superfluidity is confirmed by more extensive studies on the following issues including: the validity to extract the $\Lambda\Lambda$ bond energy of ${}^{6}_{\Lambda\Lambda}$He system by Eq.(5.1) without relevance to the rearrengement effects, the possibility of small $\Delta B_{\Lambda\Lambda}$ as a result of the three-body force repulsion, the mass-number dependence of $\Delta B_{\Lambda\Lambda}$ in double Λ hypernuclei, possible effects of $\Lambda\Lambda$-$\Sigma^-\Sigma^-$-ΞN channel coupling in the $\Lambda\Lambda$ pairing and also the Λ-superfluidity due to the $\Lambda\Sigma^-$ pairing not restricted to the $\Lambda\Lambda$ pairing, and of course the finding of new double Λ hypernuclei. For example, it is of importance to note that the inclusion of rearrangement effects on the α-particle in the $\alpha + \Lambda + \Lambda$ system suggests more attractive $\Lambda\Lambda$ interaction than $\tilde{V}^{\rm ND}_{\Lambda\Lambda}({}^1S_0)$.[52),53)]

Finally, it is worthwhile to pay attention to another possibility for fast cooling scenario. As well known, several processes of nonstandard fast cooling of DUrca type have been proposed, which work under the possible presence of nonstandard components, such as pion condensate (pion cooling), kaon condensate (kaon cooling), high proton-fraction phase (N-DUrca cooling) and quark phase (quark cooling). Among these, N-DUrca and kaon coolings are excluded from the candidates of fast cooling scenario consistent with observations, since baryon superfluidity is unlikely in these exotic phases.[54)] Also the quark cooling is excluded because of too large energy gaps exceeding several tens of MeV which absolutely supress the ν-emission. Then only the pion cooling remains as another promising candidate because there

is a strong possibility of quasibaryon superfluids due mainly to the large effective masses and pairing attraction enhanced by isobar $\Delta(1232)$ contamination.[56),57)]

Acknowledgements

The authors wish to thank S. Tsuruta and T. Tatsumi for their cooperative discussion about the cooling problem of neutron stars and also M. Wada for his helpful discussion in the use of Funabashi-Gifu baryon-baryon interaction model. This work is indebted to the financial support by the Grant-in-Aid for Scientific Research (C) from the Ministry of Education, Culture, Sports, Science and Technology (13640252, 15540244).

References

1) T. Takatsuka, S. Nishizaki, Y. Yamamoto and R. Tamagaki, *Proc. 7th Int. Conf. on "Hypernuclear and Strange Particle Physics" (HYP2000), Torino, Italy, Oct.23-27, 2000*, ed.E. Botta, T. Bressami and A. Feliciello, Nucl. Phys. **A691** (2001), 254C.
2) T. Takatsuka, S. Nishizaki, Y. Yamamoto and R. Tamagaki, Prog. Theor. Phys. Suppl. No.146 (2002), 279.
3) T. Takatsuka, *Proc. 18th Nishinomiya Yukawa Menorial Symposium on "Strangeness in Nuclear Matter", Nishinomiya, Japan, Dec. 4-5, 2003*, ed. T. Harada, A. Ohnishi and Y. Akaishi, Prog. Theor. Phys. Suppl. No.156 (2004), 84.
4) S. Tsuruta, Comments Astrophys. **11** (1986), 151.
5) S. Tsuruta, *Proc. US-Japan Joint Seminar on "The Strudure and Evolution of Neutron Stars" Kyoto, Japan, 1990*, ed. D. Pines, R. Tamagaki and S. Tsuruta (Addison-Wesley, 1992), p371.
6) S. Tsuruta, Phys. Rep. **292** (1998), 1.
7) H. Umeda, S. Tsuruta and K. Nomoto, Astrophys. J. **433** (1994), 256.
8) H. Umeda, K. Nomoto, S. Tsuruta, T. Muto and T. Tatsumi, Astrophys. J. **431**, (1994), 309.
9) S. Tsuruta, M.A. Teter, T. Takatsuka, T. Tatsumi and R. Tamagaki, Astrophys. J. **571** (2002), L143.
10) S. Tsuruta, review paper presented at *IAU Symposium on "Highly Energetic Physical Processes and Mechanisms for Emission from Astrophysical Plasmas", Sydney, Australia, July 2003*.
11) C.J. Pethick, Rev. Mod. Phys. **64** (1992), 1133.
12) M. Prakash, Phys. Rep. **242** (1994), 297.
13) D. Page and E. Baron, Astrophys. J. **354** (1990), L17.
14) D. Page and J. Applegate, Astrophys. J. **394** (1992), L17.
15) Ch. Schaab, D. Voskresensky, A.D. Sedrakian, F. Weber and M.K. Weigel, Astron. Astrophys. **321** 1997), 591.
16) D.G. Yakovlev, A.D. Kaminker, O.Y. Gnedin and P. Haensel, Phys. Rep. **351** (2001), 1.
17) D.G. Yakovlev and C.J. Pethick, Annu. Rev. Astron. Astrophys. bf 42 (2004), 169.
18) D. Blaschke, H. Grigorin and D.N. Voskresensky, Astron. Astrophys. **424** (2004), 979.
19) Mad. Prakash, Man. Prakash, J.M. Lattimer and C.J. Pethick, Astrophys. J. **390** (1992), L77.
20) T. Takatsuka and R. Tamagaki, Prog. Theor. Phys. **102** (1999), 1043; *Proc. Int. Symposium on "Physics of Hadrons and Nuclei", Tokyo, Japan, Dec. 14-17, 1998*, ed. Y. Akaishi, O. Morimatsu, M. Oka and K. Shimizu, Nucl. Phys. **A670** (2000), 222c; *Proc. APCTP Workshop on "Strangeness Nuclear Physics" (SNP'99), Seoul, Korea, Feb. 19-22,1999*, ed. I-T. Cheon, S-W. Hong and T. Matoba (World Scientific, 2000), p337.
21) T. Takatsuka, S. Nishizaki, Y. Yamamoto and R. Tamagaki, *Proc. the 1st Asian-Pasific Conference on "Few-Body Problems in Physics '99", Tokyo, Japan, Aug.23-28, 1999*, ed. S. Oryu, M. Kamimura and S. Ishikawa, Few Body Systems Suppl. **12** (2000), p108; *Proc. the 10th Int. Conf. "Recent Progress in Many-Body Theories", Seattle, USA, Sept. 10-15,*

1999, ed. R. F. Bishop, K. A. Gernoth, N. R. Walet and Y. Xian, Advances in Quantum Many-Body Theory, **3** (World Scientific, 2000), p323; *Proc. Int. Symposium on "Origin of Matter and Evolution of Galaxies 2000",Tokyo, Japan, Jan. 19-21, 2000*, ed. T. Kajino, S. Kubono, K. Nomoto and I. Tanihata, (World Scientific, 2003), p305.
22) T. Takatsuka, S. Nishizaki, Y. Yamamoto and R. Tamagaki, Prog. Theor. Phys. **105** (2001), 179.
23) S. Nishizaki, Y. Yamamoto and T. Takatsuka, Prog. Theor. Phys. **105** (2001), 607.
24) T. Takatsuka, S. Nishizaki and Y. Yamamoto, *Proc. the Int. Symposium on "Perspectires in Physics with Radioactive Isotope Beams 2000 (RIB00)", Hayama, Kanagawa, Japan, Nov. 13-16, 2000*, ed. K. Asahi, H. Sakai, I. Tanihata, T. Nakamura, C. Signorini and Th. Walcher, Eur. Phys. J. **A13** (2002), 213.
25) S. Nishizaki, Y. Yamamoto and T. Takatsuka, Prog. Theor. Phys. **108** (2002), 703.
26) M.M. Nagels, T.A. Rijken and J.T. deSwart, Phys. Rev. **D12** (1975), 744; Phys. Rev. **D15** (1977), 2547; Phys. Rev. **D20** (1979), 1633.
27) Y. Yamamoto, S. Nishizaki and T. Takatsuka, Prog. Theor. Phys. **103** (2000), 981.
28) S. Nishizaki, T. Takatsuka, N. Yahagi and J. Hiura, Prog. Theor. Phys. **86** (1991), 853.
29) S. Nishizaki, T. Takatsuka and J. Hiura, Prog. Theor. Phys. **92** (1994), 93.
30) I.E. Lagaris and V.R. Pandharipande, Nucl. Phys. **A369** (1981), 470.
31) B. Friedman and V.R. Pandharipande, Nucl. Phys. **A361** (1981), 502.
32) R.B. Wiringa, V. Fiks and A. Fabrocini, Phys. Rev. C38 (1988), 1010.
33) A. Akmal, V.R. Pandharipande and D.G. Ravenhall, Phys. Rev. **C58** (1998) 1804.
34) M. Baldo, G.F. Burgio and H.-J. Schulze, Phys. Rev. **C61** (2000), 055801.
35) I. Vidana, A. Ramos, L. Engvik and M. Hjorth-Jensen, Phys. Rev. **C62** (2000), 035801.
36) S. Balberg and N. Barnea, Phys. Rev. **C57** (1998), 409.
37) E. Hiyama, M. Kamimura, T. Motoba, T. Yamada and Y. Yamamoto, Prog. Theor. Phys. **97** (1997), 881.
38) T. Ueda, K. Tominaga, M. Yamaguchi, N. Kijima, D. Okamoto, K. Miyagawa and T. Yamada, Prog. Theor. Phys. **99** (1998), 891; Nucl. Phys. **A642** (2000), 995.
39) I. Arisaka, K. Nakagawa, S. Shinmura and M. Wada, Prog. Theor. Phys. **104** (2000), 995.
40) M. Danysz et al., Nucl. Phys. **49** (1963), 121.
41) S. Aoki et al., Prog. Theor. Phys. **85** (1991), 1287.
42) Y. Yamamoto, T. Motoba, H. Himeno, K. Ikeda and S. Nagata, Prog. Theor. Phys. Suppl. No.117 (1994), 361.
43) T. Yamada and C. Nakamoto, Phys. Rev. **C62** (2000), 034319.
44) C.B. Dover, D.J. Millener, A. Gal and D.H. Davis, Phys. Rev. **C44** (1991), 1905.
45) H. Takahashi et al., Phys. Rev. Lett. **87** (2001), 212502.
46) R. Tamagaki, Prog. Theor. Phys. **39** (1968), 91.
47) T. Takatsuka and R. Tamagaki, *Proc. the 16th Int. Conf. on "Particles and Nuclei (PANIC '02)", Osaka, Japan, Sep. 30-Oct. 4, 2002*, ed. H. Toki, K. Imai and T. Kishimoto, Nucl. Phys. **A721** (2003), 1003c.
48) T. Takatsuka and R. Tamagaki, Prog. Theor. Phys. **112** (2004), 37; *Proc. Int. Conf. on "Clustering Aspects of Nuclear Structure and Dynamics"*, ed. K. Ikeda, I. Tanihata and H. Horiuchi, Nucl. Phys. **A738** (2004), C387.
49) J.M. Lattimer, C.J. Pethick, M. Prakash and P. Haensel, Phys. Rev. Lett. **66** (1991), 2701.
50) E. Hiyama, M. Kamimura, T. Motoba, T. Yamada and Y. Yamamoto, Phys. Rev. **C66** (2002), 024007.
51) R. Tamagaki and T. Takatsuka, Soryushiron Kenkyu (Kyoto) **106** (2002), B85.
52) H. Nemura, Y. Akaishi and Y. Suzuki, Phys. Rev. Lett. **89** (2002), 142504.
53) Q.N. Usmani, A.R. Bodmer and B. Sharma, Phys. Rev. **C70** (2004), 061001.
54) T. Takatsuka and R. Tamagaki, Prog. Theor. Phys. **94** (1995), 457; Prog. Theor. Phys. **97** (1997), 345.
55) T. Takatsuka and R. Tamagaki, Prog. Theor. Phys. Suppl. No.112 (1993), 107.
56) T. Takatsuka and R. Tamagaki, Prog. Theor. Phys. **98** (1997), 393; Prog. Theor. Phys. **101** (1999), 1043.
57) R. Tamagaki and T. Takatsuka, submitted to Prog. Theor. Phys.